JOURNAL OF PHARMACEUTICAL SCIENCES

DECEMBER 1980
VOLUME 69 NUMBER 12

RESEARCH ARTICLES

Improving Intestinal Absorption of Water-Insoluble Compounds: A Membrane Metabolism Strategy

G. L. AMIDON ˣ, G. D. LEESMAN, and R. L. ELLIOTT

Received February 27, 1980, from the *School of Pharmacy, University of Wisconsin, Madison, WI 53706.* Accepted for publication June 11, 1980.

Abstract □ A strategy for improving the intestinal absorption of water-insoluble drugs was developed and tested. The strategy is based on making a soluble derivative of an insoluble compound which, in turn, is a substrate for enzymes in the surface coat of the brush border region of the microvillous membrane. Consequently, just prior to reaching the membrane, the physical properties of the diffusing species are changed from polar to nonpolar. The experimental test used two drug–drug derivative pairs, estrone–lysine estrone ester and *p*-nitroaniline–lysine *p*-nitroanilide. Wall permeabilities were determined using an external perfusion technique in the rat intestine and a laminar flow convective diffusion model for transport in the lumen. Analysis of the permeability results indicates that the derivatives have higher wall permeabilities than the parent compounds and that the microvillous surface coat may be a significant contributor to the intestinal wall resistance. Comparison of the absorption rates for estrone and the lysine estrone ester indicates that the absorption rate of the derivative could be up to five orders of magnitude greater than that for the parent compound.

Keyphrases □ Permeability—intestinal absorption of water-insoluble drugs, improved membrane permeability through synthesis of soluble derivative as prodrug □ Absorption, intestinal—water-insoluble drugs, improved membrane permeability through synthesis of soluble derivative as prodrug □ Models—intestinal absorption of water-insoluble drugs, improved membrane permeability through synthesis of soluble derivative as prodrug

Water-insoluble compounds frequently are absorbed slowly due to slow dissolution of the solid and/or a very low solution concentration, leading to a small diffusive driving force. Two approaches often are used in these cases to improve absorption: formulation and soluble derivative formation (1). The formulation approach uses physical methods such as micronization or dispersion in a soluble carrier to increase the dissolution rate of the drug product and, hence, the absorption rate. The soluble derivative (prodrug) approach attaches a solubilizing progroup (*e.g.*, phosphate or succinate) to the drug, taking advantage of the usually high solubility and dissolution rate of the derivative salt. Examples of the successful application of both approaches are available (1).

BACKGROUND

Each approach has its limitations. With the formulation approach, the maximal diffusive driving force still is limited by the low aqueous solubility of the drug. While it may be possible to maintain a supersaturated solution for a finite period of time, the supersaturation often is only a factor of two or less, which is not sufficient to ensure complete absorption for very insoluble compounds. The solubilizing progroup approach is limited by the fact that while the aqueous solubility may be increased by several orders of magnitude, the increase in solubility is coupled to a decrease in the membrane–water partition coefficient (2–4) and, consequently, results in a reduction in the membrane permeability. While the transport basis for this trade-off will be discussed in more detail, the significant point is that increased aqueous solubility usually is obtained at the expense of reduced membrane permeability. If, for oral dosage forms, the conversion back to the nonpolar drug occurs rapidly, chemically or biochemically, in the gut lumen, then the reduced membrane permeability of the drug derivative is of no consequence. However, as with the formulation approach, the diffusive transport of the drug again is limited by its low solubility.

This report discusses an approach that may avoid this compromise. The essential strategy is to make derivatives of insoluble compounds that are substrates for enzymes in the brush border region of the mucosal cells. In the next section, the biochemical background is reviewed briefly and the prodrug strategy is developed. Next, the transport processes involved are analyzed. The approach is tested experimentally using two drug–drug derivative pairs in an externally perfused rat intestine preparation. The results then are discussed in light of the transport models and the potential of this approach for improving oral absorption.

Protein Digestion and Absorption—Understanding of the digestion and absorption of proteins has increased over the past 20 years, as demonstrated by numerous reviews and symposium volumes (5–14). Prior to reaching the intestine, ingested protein is acted on by gastric and pancreatic enzymes. This process is intraluminal and reduces the protein to a mixture of free amino acids (<30%) and oligopeptides having two to six residues. This mixture is presented to the intestinal mucous membrane where an active, sodium-dependent carrier transports the free amino acids into the cell. Final hydrolysis of the remaining oligopeptides occurs along the mucous membrane and is complete so that, for practical purposes, only amino acids enter the portal circulation.

For many years, it was assumed that all of the protein was reduced to free amino acids prior to transport across the intestinal wall. Then, in a pioneering series of reports published between 1959 and 1962, Newey and Smyth (15–17) demonstrated that intraluminal hydrolysis accounted

0022-3549/80/1200-1363$01.00/0

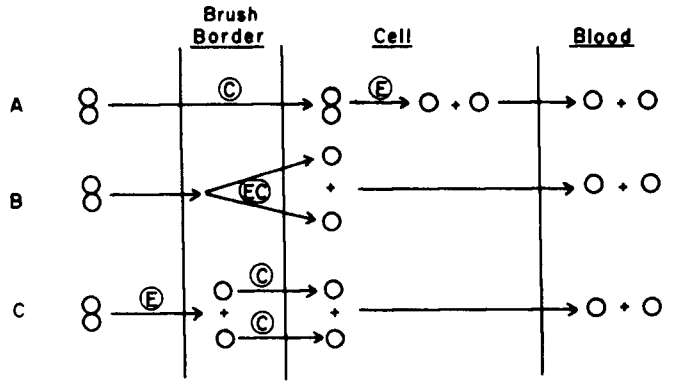

Figure 1—*Peptide absorption mechanisms. Key: A, peptide transport and cellular hydrolysis; B, coupled transport and hydrolysis; C, interfacial hydrolysis and transport;* Ⓒ, *carrier;* Ⓔ, *enzyme; and* ⒺⒸ, *enzyme–carrier system.*

for only a minor portion of the total protein hydrolyzed. In addition, they showed that small amounts of dipeptides could be absorbed into the enterocytes intact, a finding also reported by Prockop *et al.* (18). Matthews and coworkers (19, 20) made the important observation that dipeptides could be absorbed more rapidly than amino acids. This finding established that dipeptides could be transported by a mechanism independent of that used by amino acids. This result was supported by reports that patients with defective intestinal amino acid absorption, as in Hartnup's disease or cystinuria, are able to absorb dipeptides without difficulty (20, 21). Several schemes were proposed to account for the final stages of hydrolysis and absorption of oligopeptides (22–26), and these schemes include one or both of the following mechanisms (Fig. 1):

1. Hydrolysis of the small peptides by enzymes in the brush border region to amino acids. The amino acids then are transported into the cell by a unique carrier system.

2. The small peptides are reduced to (mostly) dipeptides and tripeptides by enzymes on the external surface of the cell, followed by uptake of the di- and tripeptides into the cell where the final hydrolysis takes place.

Membrane Metabolism Strategy—While the nature and specificity of the brush border region enzymes still are the subject of intensive research, the extensive enzymatic activity in the region is well established (6, 7, 11, 23). The significance of this fact, from the point of view of a prodrug strategy, is based on the solubility–partition coefficient trade-off. Increasing the membrane permeability by increasing the membrane–water partition coefficient usually results in reduced solubility, leading to an optimum partition coefficient. That is, the aqueous (luminal) phase and the nonpolar membrane phase have conflicting physical property requirements.

The basis for the prodrug solubilization strategy is as follows. If a (soluble) derivative of an insoluble (high membrane–water partition coefficient) compound can be made that is a substrate for the brush border enzymes located at the interface between the polar and nonpolar phases, then conversion back to the high partition coefficient (low aqueous solubility) compound would occur immediately adjacent to the nonpolar (membrane) sink. This, in turn, would preclude or minimize precipitation of the insoluble drug. In other words, the prodrug strategy involves the use of interfacial enzymes to convert a drug (derivative) that has desirable properties in the one phase (high solubility) to one having desirable properties in the other phase (high partition coefficient). A scheme for this approach is presented in Fig. 2.

THEORETICAL

Membrane Permeability—The transport of a solute through a composite planar membrane will be considered first. The rate of mass transport per unit area, J, is given by (using the film model) (2, 3):

$$J = P_{\text{eff}}\,\Delta C \qquad \text{(Eq. 1)}$$

$$P_{\text{eff}} = \frac{P_a P_m}{P_a + P_m} \qquad \text{(Eq. 2)}$$

$$P_a = D/\delta_a \qquad \text{(Eq. 3)}$$

$$P_m = PCD/\delta_m \qquad \text{(Eq. 4)}$$

where ΔC is the concentration difference between the two sides of the composite barrier, P_{eff} is the effective permeability coefficient, P_a is the aqueous permeability, P_m is the membrane permeability, δ_a and δ_m are the respective film thicknesses, and PC is the membrane–water partition coefficient. Equation 2 can be rewritten as:

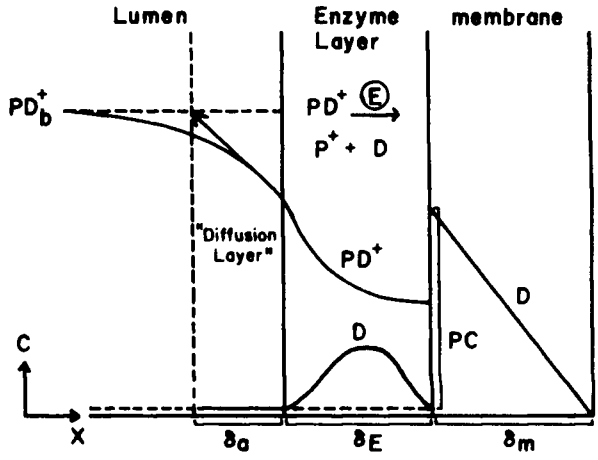

Figure 2—*Reaction diffusion model for absorption of soluble derivatives of insoluble compounds. Drug* (D) *may or may not build up in the enzyme layer. Key:* PD^+, *charged prodrug;* Ⓔ, *enzyme;* δ_a, *diffusion layer thickness;* δ_E, *enzyme layer thickness;* δ_m, *membrane thickness; and* PC, *membrane–enzyme layer partition coefficient.*

$$P_{\text{eff}} = \frac{D}{\delta_a + (\delta_m/PC)} \qquad \text{(Eq. 5)}$$

Under sink conditions, Eq. 1 becomes:

$$J = P_{\text{eff}} C_b \qquad \text{(Eq. 6)}$$

From Eq. 5, it is clear that as PC increases, P_{eff} increases and, hence, the absorption rate increases (Eq. 6). In the limit $PC \to \infty$, $P_{\text{eff}} = D/\delta_a$. However, as PC increases, a significant physical constraint must be considered: as PC increases, the aqueous solubility decreases and, as a result, C_b in Eq. 6 eventually must be replaced by C_s, the aqueous solubility:

$$J = P_{\text{eff}} C_s \qquad \text{(Eq. 7)}$$

Equation 7 represents the flux from suspensions. In this situation, increasing PC increases P_{eff} but decreases C_s to a greater extent. This trade-off leads to the existence of an optimum PC value (2, 3). Equations 5–7 are significant to a prodrug strategy since one can increase C_s but, in most cases, not without a corresponding decrease in P_{eff}[1]. However, given the preceding discussion of the interfacial (brush border) enzymatic activity, a prodrug strategy based on interfacial reconversion may be particularly effective. The transport basis for this approach is as follows. The model (Fig. 2) requires three layers with an enzymatic reaction occurring in the middle layer. The composite barrier is assumed to be planar[2], and the enzymatic reaction is assumed to be first order.

The solution for the three-layer model with a first-order reaction in the enzyme layer (rate constant = k) is:

$$J = P_R C_{A_0} \qquad \text{(Eq. 8)}$$

where P_R is a complex function of δ_w, δ_E, δ_m, K, k, and D (Fig. 2). However, a much simpler expression is obtained if it is assumed that the membrane layer is a sink for the drug and the membrane is impermeable to the (soluble) drug derivative (27). For this two-layer model, P_R from Eq. 8 becomes:

$$P_R = \frac{P_a P_E}{P_a + P_E} \qquad \text{(Eq. 9)}$$

with:

$$P_E = \alpha D \tanh(\alpha \delta_E) \qquad \text{(Eq. 10)}$$

$$\alpha^2 = k/D \qquad \text{(Eq. 11)}$$

[1] See Ref. 4 for examples where this is not the case.

[2] The error involved with this assumption for a cylinder having a radius of 0.2 cm is only 2–3% (27).

where k is the first-order reaction rate in the enzyme layer and P_a is D/δ_a. Note that:

$$\lim_{k\to 0} P_R = 0 \quad \text{and} \quad \lim_{k\to\infty} P_R = P_a$$

The most significant point regarding Eqs. 8–11 is that C_{A_0} is the concentration of the soluble drug derivative and that the membrane–aqueous solution partition coefficient does not enter into the equation. If the enzymatic reaction is fast (large k), the flux of the soluble drug derivative can be orders of magnitude greater than that of the insoluble drug.

Convective Diffusion Model—The experimental test system used a perfused rat intestine. Consequently, a model accounting for both convection and diffusion in a tube is required. The most appropriate model with the present experimental procedure is a laminar flow model (28). The solution to the convective diffusion problem for steady flow in a cylindrical tube with a permeable wall gives (27):

$$C_m/C_0 = \Sigma M_n \exp(-\beta_n^2 Gz) \qquad \text{(Eq. 12)}$$

where:

C_m = outlet (cup-mixing) concentration
C_0 = inlet concentration
$Gz = \pi DL/2Q$
D = aqueous diffusivity of the solute
L = length of the perfused intestine
Q = flow rate

and the M_n and β_n values are functions of the dimensionless (membrane) wall permeability, P_w^*, defined as:

$$P_w^* = \frac{P_w R}{D} \qquad \text{(Eq. 13)}$$

where R is the radius of the intestine.

The P_w value is defined by the boundary condition at the tube wall:

$$-D\left.\frac{\partial C}{\partial r}\right|_{r=R} = P_w C_w \qquad \text{(Eq. 14)}$$

where $C_w = C(R,z)$ is the wall concentration. The results in this study were analyzed using the laminar flow model, although other models could be applied to the data (28). It is important to note that P_w (or P_w^*) does not contain any contribution from the luminal diffusion of the drug. That is, there is no diffusion layer in the model; the luminal diffusion of the drug is accounted for by solution of the appropriate transport equation (27). For passively absorbed compounds, P_w^* is equal to P_m^* in Eq. 4; for the reactive compounds, P_w^* is equal to P_k^* of Eq. 10. Consequently, in interpreting the results, P_w^* must be interpreted appropriately.

The preceding analysis can be related to a pharmacokinetic analysis through a mass balance on the tube. This approach gives:

$$dm/dt = C_0(1 - C_m/C_0)Q \qquad \text{(Eq. 15)}$$

where dm/dt is the mass transported across the absorbing surface per unit time and can be computed directly from the perfusion results. A pharmacokinetic analysis would give $dm/dt = k_{abs}VC_0$, where V is the volume of the intestinal segment. Hence:

$$k_{abs} = (1 - C_m/C_0)Q/V \qquad \text{(Eq. 16)}$$

where C_m/C_0 is a function of the wall permeability (Eq. 12) and Q/V is the residence time of the fluid in the perfused segment. Equation 16 indicates that k_{abs} increases as Q/V increases. That is, the fluid stays in the intestinal segment longer and increases as C_m/C_0 decreases, *i.e.*, as P_w^* or Gz increases.

EXPERIMENTAL

Materials—The drug–prodrug pairs used were p-nitroaniline[3]–L-lysine p-nitroanilide[3] and [^{3}H]estrone[4]–[^{3}H]estrone-3′-L-lysine ester (I). [^{14}C]Polyethylene glycol[4] was used as a volume marker. [^{3}H]Estrone-3′-L-lysine ester was synthesized from [^{3}H]estrone and L-lysine. The synthesis and physicochemical properties of I will be the subject of a subsequent report (29).

Perfusion Experiments—Male Holtzman rats (300–350 g), fasted 12–18 hr, were anesthetized intramuscularly (gluteal muscle) with a 50% urethan solution (150 mg/100 g). A midline longitudinal incision was made in the abdomen, and a glass cannula was placed 2 and 10 cm distal to the ligament of Treitz. A pump[5] was used for perfusion at flow rates of 0.05–1.2 ml/min. Glass tubing was used throughout. [^{14}C]Polyethylene glycol was used as the volume marker. Volume changes rarely exceeded 3%.

An isotonic Sorensen phosphate buffer (pH 6.72) was used. The intestine was perfused first with buffer for 30 min and then for 30–60 min (until steady state) with drug solution. At the conclusion of the experiment, the animal was sacrificed. The intestine was excised and the length of the intestine from cannula to cannula was measured. The radius was calculated from the volume of the excised segment.

Assay—p-Nitroaniline and L-lysine p-nitroanilide were assayed spectrometrically at 375 and 315 nm, respectively. [^{3}H]Estrone, [^{3}H]lysine estrone ester, and [^{14}C]polyethylene glycol were assayed by liquid scintillation. In experiments with lysine p-nitroanilide, the effluent solution was analyzed for both lysine p-nitroanilide and p-nitroaniline. Measurable amounts of p-nitroaniline were not detected in any experiments with lysine p-nitroanilide.

Table I—Coefficients and Exponents for Eq. 19

n	${}^0M_n$	${}^0\beta_n$
1	0.81905	2.7044
2	0.09753	6.6790
3	0.03250	10.6734
4	0.01544	14.6712
5	0.00879	18.6699

RESULTS AND DISCUSSION

The experimental design was such that luminal reconversion (either biochemical or chemical) of the drug derivatives would not be significant, and none was observed. The conditions also maximized the possible attainment of laminar flow in the lumen (28). The results were analyzed using the method of Elliott *et al.*[6], interpreting the wall permeability appropriately (Eq. 4 or 10). The approximate wall permeability, ${}^0P_w^*$, was calculated from:

$$\frac{1}{{}^0P_w^*} = \frac{1}{P_{eff}^*} - \frac{1}{{}^0P_{aq}^*} \qquad \text{(Eq. 17)}$$

where:

$${}^0P_{aq}^* = \frac{\ln(C_m/C_0)\exp}{-4Gz} \qquad \text{(Eq. 18)}$$

and:

$${}^0P_{aq}^* = -\left[\sum_{n=1}^{5} {}^0M_n \exp(-{}^0\beta_n^2 Gz)\right] \Big/ 4Gz \qquad \text{(Eq. 19)}$$

The coefficient and exponents in Eq. 19 are given in Table I. This approach is equivalent to the diffusion layer approach but with the diffusion layer thickness calculated *a priori* (27). The exact expression for the diffusion layer thickness is:

$$\delta/R = \frac{1}{p_{aq}^*} = \frac{-4Gz}{\Sigma M_n \exp(-\beta_n^2 Gz)} - \frac{1}{P_w^*} \qquad \text{(Eq. 20)}$$

using the M_n and β_n values that are appropriate to the wall permeability, P_w^*. While P_w^* is unknown, analysis of the model shows that δ/R is only slightly dependent on P_w^*; hence, Eq. 19, which is appropriate for sink conditions [$P_w^* = \infty$ or $C(R,z) = 0$], provides a good estimate. A small correction then can be applied to the estimated ${}^0P_w^*$ from Eq. 17 to obtain P_w^* (27).

Wall Permeabilities—The experimental results and the calculated

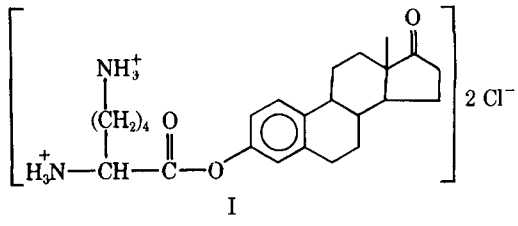

I

[3] U.S. Biochemical Corp., Cleveland, Ohio.
[4] New England Nuclear, Boston, Mass.
[5] Harvard.
[6] R. L. Elliott, G. L. Amidon, and E. N. Lightfoot, *J. Theor. Biol.*, in press.

Table II—Results for Estrone Experiments

C_m/C_0	Gz	P^*_{eff}	${}^0P^*_{aq}$	${}^0P^*_m$ [a]
0.909	0.00891	2.67	4.64	6.31
0.847	0.0178	2.33	3.71	6.27
0.739	0.045	1.68	2.81	4.17
0.784	0.036	1.68	2.99	3.87
0.92	0.0094	2.21	4.56	4.31
0.889	0.0086	3.42	4.70	12.5
0.908	0.0089	2.71	4.64	6.50
0.903	0.0092	2.77	4.59	6.98
0.864	0.012	3.04	4.21	10.9
0.882	0.01	3.13	4.47	10.5
0.921	0.0074	2.78	4.94	6.34
0.751	0.035	2.04	3.02	6.33
0.659	0.086	1.21	2.39	2.45
0.762	0.033	2.05	3.07	6.24
0.683	0.082	1.16	2.41	2.23
0.814	0.021	2.44	3.52	8.04
0.762	0.041	1.65	2.88	3.89

[a] Average ${}^0P^*_m = 6.3$, $s = 2.9$, and $SEM = 0.7$.

permeabilities are given in Tables II–V. Table VI presents a summary of the results, including the correction factors that are required to obtain an estimate of the (laminar flow) wall permeability. In analyzing the data in Tables II–V, the negative membrane permeabilities were omitted. In these cases, P^*_{eff} is greater than the calculated ${}^0P^*_{aq}$, predominantly with the reactive enzyme substrates having high P^*_w values. The possible reasons for this result are as follows. With the laminar flow model at any given Gz value, C_m/C_0 approaches a finite limit as $P^*_w \to \infty$. Since $P^*_{aq} \doteq 3$ as P^*_w increases above this value, the method loses sensitivity to P^*_w; that is, small changes in the experimentally determined C_m/C_0 values give rise to widely different P^*_w values. Experimental variation and error then can give rise to C_m/C_0 values that actually are lower than the values that the model can predict. In addition, the flow in the intestine in any given experiment may depart from laminar flow. Such mixing decreases C_m/C_0 below that expected by the model for very permeable compounds.

Since the variables of the flow rate and the length of the perfused intestine both are incorporated into the dimensionless variable Gz and since P^*_w should be independent of Gz[7] (27), regression analysis on ${}^0P^*_w$ *versus* Gz was performed. The results for estrone are shown in Fig. 3, and the regression equation is:

$${}^0P^*_w = 8.57 - 80.5Gz \qquad \text{(Eq. 21)}$$

$$n = 17 \quad s = 2.14 \quad r = 0.69$$

While there is considerable scatter and the variance does not appear to be constant, an increase in ${}^0P^*_w$ with decreasing Gz (increasing flow rate) is suggested by the data. A possible explanation might be that increasing the flow rate increases the diameter of the intestine. Since the Graetz number is independent of the radius[8] ($Gz = \pi DL/2Q$), the result is likely to be due to a change in the wall characteristics with the flow rate. For example, the surface coat on the microvillous membrane may become thinner as the radius increases, and, hence, the resistance would be lower.

Parent Compound Permeabilities—The wall permeabilities, P^*_w, for *p*-nitroaniline and estrone are interpreted following Eq. 4 as:

$$P^*_w = P^*_m = \frac{P_m R}{D} = PCR/\delta_m \qquad \text{(Eq. 22)}$$

Thus, a direct proportionality of P^*_w with the partition coefficient is expected. The octanol–water partition coefficients are ~25 and 600, respectively (30, 31). Hence, the wall permeabilities (P^*_w) of 6 and 3 are in the correct order, *i.e.*, estrone > *p*-nitroaniline. Since the aqueous resistance has been accounted for, the fact that the wall permeability ratio of estrone $[P^*_w(E_1)]$ to *p*-nitroaniline $[P^*_w(\text{pNA})]$ is 2 while the partition coefficient ratio is 25, combined with the model:

$$\frac{P^*_w(E_1)}{P^*_w(\text{pNA})} = \frac{P_w(E_1)}{P_w(\text{pNA})} = \frac{PC(E_1)}{PC(\text{pNA})} \qquad \text{(Eq. 23)}$$

clearly suggests that the model for the wall permeability must be improved. Some factors to be considered include: (*a*) the octanol–water partition coefficient does not reflect the physiological situation, (*b*) the aqueous phase and the membrane phase diffusivities differ greatly, and (*c*) the wall resistance term is composed of more than just a term for the nonpolar phase. The first factor undoubtedly is true, but it certainly is not the only (or perhaps major) reason. The effect of differing membrane diffusivities is analyzed as follows. The convective mass transport model used for analysis of the data was solved subject to the first-order boundary condition:

$$-\left.\frac{\partial C}{\partial r}\right|_{r=R} = \frac{P_w R}{D} C_w = P^*_w C_w \qquad \text{(Eq. 24)}$$

[7] The analysis is based on ${}^0P^*_w$ rather than P^*_w since the variation of the correction factor with Gz is small.

[8] The Gz value does not depend on R because the R dependence of the residence time cancels the R dependence of the radial penetration time when the flow rate is held constant.

Table III—Results of Lysine Estrone Experiments [a]

C_m/C_0	Gz	P^*_{eff}	${}^0P^*_{aq}$	${}^0P^*_m$ [b]
0.781	0.0062	9.96	5.25	−11.1
0.84	0.0057	7.64	5.41	−18.5
0.958	0.005	2.14	5.66	3.45
0.883	0.0061	5.09	5.28	144.0
0.955	0.0054	2.13	5.51	3.47
0.924	0.0061	3.23	5.28	3.36
0.661	0.0062	16.6	5.25	−7.67
0.914	0.0059	3.81	5.34	13.2

[a] Negative values were not included in the statistics (see text). Average ${}^0P^*_m = 34$, $s = 62$, and $SEM = 28$.

Table IV—Results for *p*-Nitroaniline Experiments [a]

C_m/C_0	Gz	P^*_{eff}	${}^0P^*_{aq}$	${}^0P^*_m$ [b]
0.892	0.0137	2.08	4.03	4.31
0.768	0.0055	11.9	5.47	−10.0
0.888	0.016	1.85	3.83	3.59
0.696	0.0064	14.1	5.19	−8.21
0.885	0.016	1.90	3.83	3.79
0.91	0.016	1.47	3.83	2.39
0.916	0.0137	1.60	4.03	2.65
0.912	0.017	1.35	3.76	2.11
0.892	0.0137	2.08	4.03	4.31
0.888	0.016	1.85	3.83	3.59

[a] Negative values were not included in the statistics (see text). [b] Average ${}^0P^*_m = 3.3$, $s = 0.9$, and $SEM = 0.3$.

Table V—Results for Lysine *p*-Nitroanilide Experiments [a]

C_m/C_0	Gz	P^*_{eff}	${}^0P^*_{aq}$	${}^0P^*_m$
0.772	0.0185	3.49	3.66	75.6
0.746	0.0145	5.05	3.96	−18.3
0.767	0.012	5.52	4.21	−17.7
0.878	0.017	1.91	3.76	3.88
0.775	0.012	5.31	4.21	−20.3
0.806	0.012	4.49	4.21	−67.5
0.856	0.013	2.99	4.10	11.0
0.807	0.014	3.82	4.00	86.0
0.635	0.01	11.3	4.47	−7.38
0.881	0.01	3.16	4.47	10.8
0.915	0.01	2.22	4.47	4.41
0.576	0.016	8.61	3.83	−6.92
0.858	0.011	3.48	4.33	17.6
0.852	0.011	3.64	4.33	22.7
0.915	0.0096	2.31	4.53	4.72
0.791	0.0096	6.10	4.53	−17.6

[a] Negative values are not included in the statistics (see text). [b] Average ${}^0P^*_m = 26$, $s = 32$, and $SEM = 11$.

Table VI—Wall Permeability Values for Compounds Studied

Compound	${}^0P^*_w$ [a]	γ [b]	P^*_w [c]
Estrone	6.3	0.92	6
Estrone-3′-L-lysine ester	34	0.87	30
p-Nitroanilide	3.3	0.93	3
L-Lysine *p*-nitroanilide	26	0.87	23

[a] Approximate (dimensionless) wall permeability (Eq. 17). [b] Correction factor (27). [c] Estimated wall permeability, $P^*_w = \gamma {}^0P^*_w$, for laminar flow model (Eqs. 12 and 13).

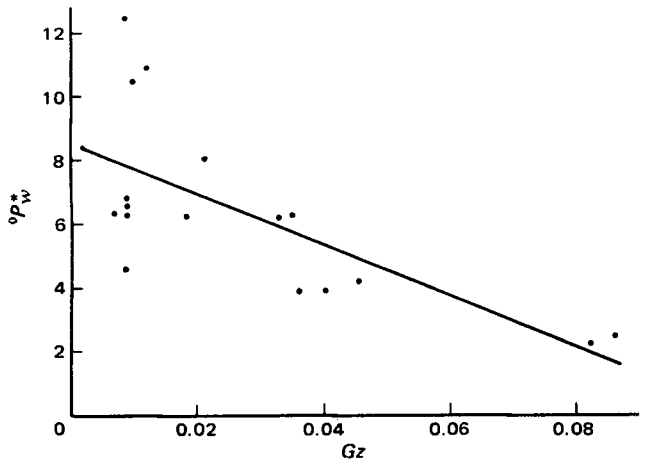

Figure 3—*Plot of the wall permeability,* $^0P^*_w$, *for estrone as a function of the Graetz number* (Gz).

or:

$$-D\left.\frac{\partial C}{\partial r}\right|_{r=R} = P_w C_w = J_w \qquad \text{(Eq. 25)}$$

where J_w is the flux at the wall, P_w is the permeability of the wall, and D is the aqueous diffusivity. A membrane model for the wall would give:

$$J_w = \frac{PCD_m C_w}{\delta_m} \qquad \text{(Eq. 26)}$$

where D_m and δ_m are the membrane parameters. Hence:

$$P_w = \frac{PCD_m}{\delta_m} \qquad \text{(Eq. 27)}$$

and:

$$P^*_w = \frac{PCD_m R}{D\delta_m} \qquad \text{(Eq. 28)}$$

Thus, the ratio of wall permeabilities is:

$$\frac{P^*_w(E_1)}{P^*_w(\text{pNA})} = \frac{PC(E_1)}{PC(\text{pNA})} = \frac{D_m(E_1)}{D_m(\text{pNA})} \qquad \text{(Eq. 29)}$$

assuming equal aqueous diffusivities for estrone and *p*-nitroaniline but not equal membrane permeabilities. Thus, the small ratio of dimensionless wall permeabilities may be due in part to a significantly lower D_m for estrone.

The third factor, an additional wall resistance term, is suggested by the presence of a surface coat on the microvillous membrane (32). If this glycoprotein layer is the major contributor to the membrane resistance, then the simple membrane model again would give Eq. 4, but, in this case, the partitioning would be into a more polar environment and the diffusivities of estrone and *p*-nitroaniline could be substantially different in the glycoprotein layer. Hence, both factors may reduce the permeability ratio.

Reactive Solute Permeabilities—For the reactive solutes, lysine estrone and lysine *p*-nitroanilide, the wall permeability may be interpreted following Eq. 10. Two limits are of interest: high reactivity, where $\alpha\delta_E > 1$ ($\tanh \alpha\delta_E \doteq 1$), for which:

$$P_w = \alpha D \qquad \text{(Eq. 30)}$$

or:

$$P^*_w = \alpha R \qquad \text{(Eq. 31)}$$

and low reactivity, where $\alpha\delta_E \ll 1$ ($\tanh \alpha\delta_E \doteq \alpha\delta_E$), for which:

$$P_w = \alpha^2 D\delta_E \qquad \text{(Eq. 32)}$$

or:

$$P^*_w = \alpha^2\delta^R_E \qquad \text{(Eq. 33)}$$

The lysine estrone–lysine *p*-nitroanilide permeability ratio $[P^*_w(\text{LE}_1)/P^*_w(\text{LpNA})]$ becomes:

$$\frac{P^*_w(\text{LE}_1)}{P^*_w(\text{LpNA})} = \frac{k_{\text{LE}_1}}{k_{\text{LpNA}}} \qquad \alpha\delta_E > 1 \qquad \text{(Eq. 34)}$$

and:

$$\frac{P^*_w(\text{LE}_1)}{P^*_w(\text{LpNA})} = \left(\frac{k_{\text{LE}_1}}{k_{\text{LpNA}}}\right)^2 \qquad \alpha\delta_E \ll 1 \qquad \text{(Eq. 35)}$$

While the membrane enzymes involved in the hydrolysis reactions are not well characterized, kinetic results for trypsin have shown amides to be much poorer substrates than the corresponding esters (33). Consequently, the similar permeability values for LE_1 and LpNA are not likely to be explained in this manner.

As with the passively absorbed compounds, it may be that the surface coat on the microvillous membrane serves as an additional resistance. In this case, the enzymes at the interface (and perhaps to some extent in the surface coat) would provide the effective sink rather than the partitioning into the membrane. Although the scatter in the data is considerably larger for the reactive substrates, the results clearly indicate that the effective wall permeability of the reactive substrates is higher than the corresponding passively absorbed compounds by a factor of five to 10. Based on the suggested interpretation, the reason could be that the effective thickness of the surface coat is smaller for the reactive substrates.

While the interpretation of the permeability values clearly requires more experimental work, the most important point to be obtained from these results is that the derivatives have permeabilities at least as great as those of the parent compounds. Consequently, they are absorbed very efficiently, even though the compounds have smaller diffusivities and much higher polarity (lower partition coefficients) due to the protonated α- and ϵ-amino groups. Thus, an equal or greater effective permeability has been achieved along with much higher aqueous solubility. Since absorption of the intact derivatives is unlikely, hydrolysis at the membrane interface apparently is very effective.

The results also imply that the interfacial reaction is as fast or faster than aqueous diffusion or diffusion through the surface coat since the results approach (and exceed) the value that would be obtained if sink conditions ($P^*_w = \infty$) prevail. Furthermore, lysine *p*-nitroanilide is relatively stable in solution and yet is absorbed very efficiently. This finding suggests that the hydrolysis of amides is at least as fast as luminal diffusion. Consequently, amide derivatives of amines, which otherwise are too stable for chemical reconversion to be effective, may be effective using this strategy.

Absorption Rate—To illustrate further the potential of this approach, the results of the estrone and lysine estrone experiments are graphed in Fig. 4 following Eq. 15 in the form:

$$\log dm/dt = \log[(1 - C_m/C_0)Q] + \log C_0 \qquad \text{(Eq. 36)}$$

A single line is drawn through the estrone and lysine estrone data since their effective permeabilities are nearly the same. That is, at the same flow rate, the fraction absorbed $(1 - C_m/C_0)$ is the same, provided that C_0 is below the saturation concentration. When saturation is reached, $C_0 = C_s$ and the amount absorbed per unit time levels off at a constant value.

On the other hand, for lysine estrone, the mass transfer per unit time increases until the solubility of 0.3 *M* is reached (29). The result is that the amount of lysine estrone absorbed per unit time could be about five orders of magnitude greater than that for estrone (note that Fig. 4 is a log–log plot).

Clearly, many questions remain to be investigated, both with respect

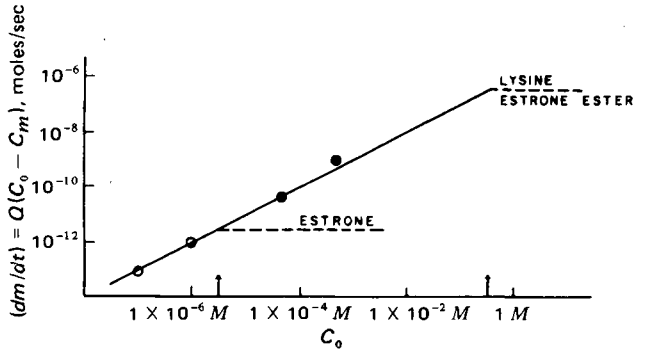

Figure 4—*Amount of drug absorbed per unit time* (dm/dt) *as a function of the initial perfusing concentration* (C_0) *for estrone and lysine estrone. Key:* ○, *estrone;* ●, *lysine estrone;* ↑, *solubilities; and* – –, *theoretical limits.*

to the absorption mechanism and to the actual effectiveness of the strategy in normal physiological situations. However, the results obtained to date strongly suggest that the biochemical strategy offers a new approach with great potential for improving drug product efficacy.

CONCLUSION

A biochemical strategy for improving the absorption of water-insoluble drugs has been tested and shown to have potential for increasing the absorption rates of insoluble compounds by several orders of magnitude. The strategy is based on the use of the enzymes in the interfacial brush border region of the mucosal cells to effect a conversion of the soluble derivative back to the insoluble, high partition coefficient parent compound. Since the aqueous luminal fluid and nonpolar membrane phases have conflicting physical property requirements, the interfacial reaction is, in effect, being used to change the physical properties of a compound from one having desirable aqueous (luminal) properties to one having desirable membrane permeation properties.

Results on two drug–drug derivative pairs, estrone–lysine estrone and *p*-nitroaniline–lysine *p*-nitroanilide, show that the effective intestinal membrane permeability of the derivatives is actually five to 10 times greater than that of the parent compounds. Since the derivatives are significantly more polar than the parent compound, the results indicate that the effective permeability associated with the interfacial enzymatic reaction is not a determining resistance. Thus, the usual physical property compromise necessary to obtain efficient drug absorption by other strategies is avoided. Analysis of the permeability data for both the parent compounds and derivatives suggests that the surface coat on the microvillous membrane may be an important resistance in the absorption process. The apparent residual dependence of the wall permeability on Gz also may be due to a thinning of this coat as *Gz* decreases. In addition, the higher wall permeabilities of the derivatives compared to the parent compounds may be due in part to hydrolysis partially occurring in this layer, reducing its effective thickness.

Analysis of the data in terms of the absorption rate (mass transport per unit time) indicates that an improvement of several orders of magnitude is possible. For lysine estrone–estrone, a two to three order of magnitude increase has been demonstrated, with a four or five order of magnitude increase possible. Given the high solubility, dissolution rate, and permeability of lysine estrone, the biochemical strategy appears to be capable of significantly improving the absorption of water-insoluble drugs.

REFERENCES

(1) "Solubilization," S. H. Yalkowsky, Ed., Dekker, New York, N.Y., 1980.

(2) G. L. Flynn and S. H. Yalkowsky, *J. Pharm. Sci.*, **61**, 838 (1972).

(3) S. H. Yalkowsky and G. L. Flynn, *ibid.*, **62**, 210 (1973).

(4) G. L. Amidon, in "Solubilization," S. H. Yalkowsky, Ed., Dekker, New York, N.Y., 1980.

(5) W. S. Saari, M. B. Freedman, R. D. Hartman, S. W. King, A. W. Raab, W. C. Randall, E. L. Englehardt, and R. Hirschmann, *J. Med. Chem.*, **21**, 746 (1978).

(6) "Peptide Transport and Hydrolysis," Ciba Foundation Symposium 50, Elsevier, Amsterdam, The Netherlands, 1977.

(7) "Peptide Transport in Bacteria and Mammalian Gut," Ciba Foundation Symposium 4, Elsevier, Amsterdam, The Netherlands, 1972.

(8) M. D. Hellier and C. D. Holdsworth, in "Intestinal Absorption in Man," I. McColl and G. E. Sladen, Eds., Academic, New York, N.Y., 1975, pp. 143–186.

(9) M. H. Sleisenger and Y. S. Kim, *N. Engl. J. Med.*, **300**, 659 (1979).

(10) D. M. Matthews, *Gastroenterology*, **73**, 1267 (1977).

(11) D. M. Matthews, *Physiol. Rev.*, **55**, 537 (1975).

(12) D. M. Matthews and S. A. Adibi, *Gastroenterology*, **71**, 151 (1976).

(13) D. M. Matthews, in "Peptide Transport in Protein Nutrition," D. M. Matthews and J. W. Payne, Eds., North-Holland, Amsterdam, The Netherlands, 1975, pp. 61–146.

(14) G. M. Gray and H. L. Cooper, *Gastroenterology*, **61**, 535 (1971).

(15) H. Newey and D. H. Smyth, *J. Physiol.*, **145**, 48 (1959).

(16) *Ibid.*, **152**, 367 (1960).

(17) *Ibid.*, **164**, 527 (1962).

(18) D. J. Prockop, H. R. Keiser, and A. Smoerdsma, *Lancet*, **2**, 527 (1962).

(19) I. L. Craft, D. Geddes, C. W. Hyde, I. J. Wise, and D. M. Matthews, *Gut*, **9**, 425 (1968).

(20) D. M. Matthews, I. L. Craft, D. M. Geddes, I. J. Wise, and C. W. Hyde, *Clin. Sci.*, **35**, 415 (1968).

(21) A. M. Asatoor, B. Cheng, K. D. G. Edwards, A. F. Lant, D. M. Matthews, M. D. Milne, F. Navab, and A. J. Richards, *Gut*, **11**, 380 (1970).

(22) A. M. Ugolev, in "Peptide Transport in Bacteria and Mammalian Gut," Ciba Foundation Symposium 4, Elsevier, Amsterdam, The Netherlands, 1972, pp. 123–127.

(23) A. M. Ugolev, in "Biomembranes," vol. 4A, D. M. Smyth, Ed., Plenum, New York, N.Y., 1974, pp. 285–362.

(24) A. M. Ugolev, in "Peptide Transport and Hydrolysis," Ciba Foundation Symposium 50, Elsevier, Amsterdam, The Netherlands, 1977, pp. 221–238.

(25) D. M. Matthews, *Physiol. Rev.*, **55**, 595 (1975).

(26) A. N. Radhakrishnan, in "Peptide Transport and Hydrolysis," Ciba Foundation Symposium 50, Elsevier, Amsterdam, The Netherlands, 1977, p. 50.

(27) R. L. Elliott, Ph.D. thesis, University of Wisconsin, Madison, Wis., 1979.

(28) G. L. Amidon, J. Kou, R. L. Elliott, and E. N. Lightfoot, *J. Pharm. Sci.*, **69**, 1369 (1980).

(29) G. D. Leesman, Ph.D. thesis, University of Wisconsin, Madison, Wis., 1980.

(30) N. F. H. Ho, J. Y. Park, W. Morozowich, and W. I. Higuchi, in "Design of Biopharmaceutical Properties through Prodrugs and Analogs," E. B. Roche, Ed., APhA Academy of Pharmaceutical Sciences, Washington, D.C., 1977, p. 155.

(31) A. Leo, C. Hansch, and D. Elkins, *Chem. Rev.*, **71**, 525 (1971).

(32) J. S. Trier, in "Alimentary Canal," vol. 3, "Handbook of Physiology," American Physiological Society, Washington, D.C., 1968, p. 1138.

(33) B. Keil, in "The Enzymes," vol. 3, P. D. Boyer, Ed., Academic, New York, N.Y., 1971, p. 266.

ACKNOWLEDGMENTS

Supported by The Upjohn Co., Biomedical Research Support Grant SO 7RR05456-17, and GM 27680.

The authors thank Ms. Shannon Sullivan and Mr. James Kou for assistance with portions of this work.